

## COMMISSIONING OF A DECAY-SPECTROSCOPY STATION FOR THE 9 MV TANDEM ACCELERATOR

Sebastian TOMA<sup>1, 2</sup>, Tiberiu SAVA<sup>3</sup>, Dan Gabriel GHIȚĂ<sup>4</sup>, Nicolae Marius MĂRGINEAN<sup>2</sup>, Gheorghe CĂTA-DANIL<sup>1</sup>, Nicolae-Victor ZAMFIR<sup>4</sup>, Dorin MOISĂ<sup>3</sup>

*A new experimental setup for decay spectroscopy has been commissioned at the 9-MV Tandem Accelerator facility of IFIN-HH. It consists of a tape-transport station (moving tape collector - MTC) which separates nuclei of interest from other nuclear species produced in fusion-evaporation reactions, coupled to an array of HPGe clover detectors and digital data acquisition in a reduced-background area. Two types of experiments have been performed to assess the MTC performances.*

**Keywords:** tape-transport station, decay spectroscopy, HPGe detectors, digital data acquisition.

### 1. Introduction

Our understanding of the structure of atomic nuclei relies on measured nuclear properties confronted against theoretical model predictions. Measurable quantities such as  $\gamma$ -ray energies and intensities following transitions between two discrete levels lead to experimental excitation spectra, lifetimes of nuclear states, directly related to the eigenvectors and eigenvalues of the nuclear quantum problem [1].

At the Bucharest 9 MV Tandem Accelerator facility [2][3], these types of information are, in most cases, extracted via *in-beam*  $\gamma$ -ray spectroscopy experiments using fusion-evaporation reactions [4] and employs several measurement techniques, with a focus on lifetime measurements of excited nuclear states [5][6]. Fusion-evaporation is a high-multiplicity reaction mechanism which favors the population of mainly high-spin states in neutron-deficient nuclei, and their subsequent  $\gamma$  decays follow the yrast line, restricting the available information.

---

<sup>1</sup> Department of Physics, University POLITEHNICA of Bucharest, Romania, e-mail: sebastian.toma@physics.pub.ro

<sup>2</sup> Department of Nuclear Physics, “Horia Hulubei” Institute for Physics and Nuclear Engineering, Romania, e-mail: sebastian.toma@nipne.ro

<sup>3</sup> Department of Tandem Accelerators, “Horia Hulubei” Institute for Physics and Nuclear Engineering, Romania

<sup>4</sup> ELI-NP, “Horia Hulubei” Institute for Physics and Nuclear Engineering, Romania

Alternate population mechanisms are required to access low-spin non-yrast states, and one possibility is the use of the  $\beta$  decay mechanism, with the nucleus of interest obtained as the daughter-nucleus of a  $\beta$ -decaying parent. The latter is the focus of the work reported in the present paper.

The current approach to obtaining the  $\beta$ -decaying parent-nuclei makes use of a *pulsed-beam* [7]: a beam-on period is used to start a clock, i.e. to define the parent-nucleus population at time  $t=0$ , then the beam is switched-off for a period during which  $\gamma$ -ray transitions from the daughter are detected and recorded. *In-beam* experiments require thick or backed targets and, considering the multiple exit channels from a fusion-evaporation reaction [4], all nuclei produced in the reaction will remain in the target. These can further decay, contaminating data over the course of an experiment. It is a fundamental experimental requirement to separate the parent-nuclei of interest from the rest of the exiting channels.

In this work we present a new experimental setup, recently installed and commissioned at IFIN-HH, dedicated for the study of  $\beta$ -decay daughters of nuclei produced in heavy-ion-induced reactions from the 9-MV Tandem Accelerator. It consists of a tape-transport system based on the Yale WNSL design [8], improved in terms of speed and controllability, coupled to a high-efficiency HPGe clover [9] detector array using digital data acquisition. Special care was taken to ensure the system can be maintained in vacuum of order  $10^{-7}$  -  $10^{-6}$  mbar. Our geometry allows to perform  $\gamma$  spectroscopy in a reduced-background environment. The principle of the method and hardware description are accompanied by results from the commissioning test, while the experimental limits of the setup are explored in the context of using  $\alpha$ -induced reactions for half-life measurements.

## 2. Experimental Setup Description

The new experimental setup, called “The Moving Tape Collector” (abbreviated as “MTC” from now on), allows the production and separation of parent-nuclei, and measurements on their resulting daughter-nuclei, strictly in an accelerator environment. A brief description of the MTC is shown in Figure 1. Optimum beam-target combinations are obtained using computer codes such as PACE [13][14], COMPA[15] and NRV[17], providing channel production cross-sections, as well as reaction kinematics, i.e. recoil kinetic energy and angular distribution. Estimates for the isotopically-enriched self-supported target thickness are obtained using TRIM [16] and COMPA [15] and take into account the recoil energy from the previous step. The recoiling reaction products are then extracted downstream of the target due to their kinetic energy relative to the target’s thickness, each with a specific angular distribution. A  $\sim$ 2.5 mm thick and  $\sim$  2 mm wide Tantalum beam plug (stopper) placed after the target acts as a fragment separator: the unreacted primary ion beam is stopped on the plug, while most

fusion-evaporation products bypass it and are further implanted in a 16 mm Kapton tape. A first optimization step is done by adjusting the target-tape distance (typically between 2 and 6 cm) to favor the outgoing channel (parent-nucleus) of interest.

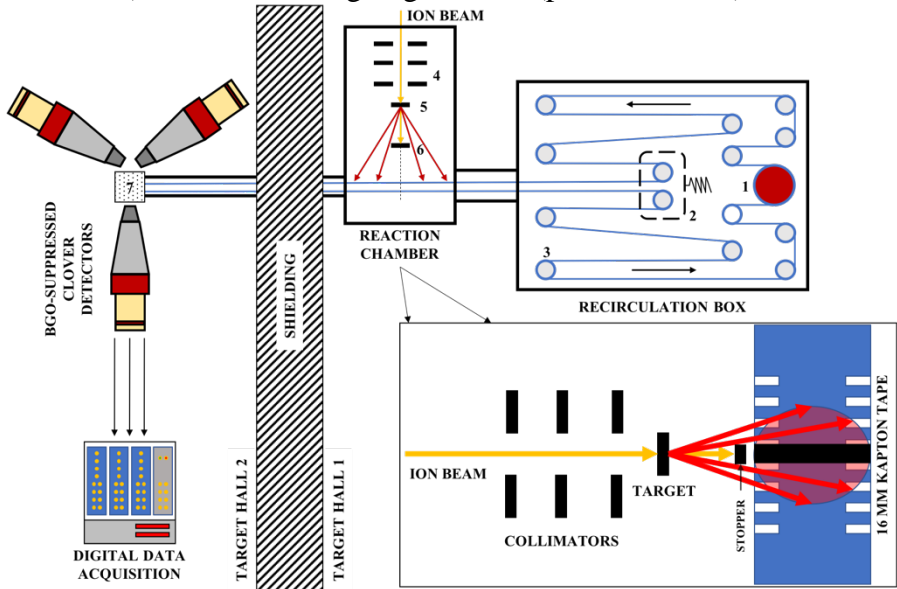


Fig. 1 – Schematic representation of the tape-transport system with a zoom-in of the reaction chamber and implantation point

1 – Sprocket wheel, 2 – Tensioning platform, 3 – Roller pulley, 4 – Collimators, 5 – Self-supported Target, 6 – Beam plug (Stopper), 7 – Measurement Point. See text for details

The tape transports the implanted radioactivity  $\sim 2.76$  m to a shielded measurement area at regular intervals, chosen according to the parent-nucleus half-lives. This is done by using a stepper motor to drive a sprocket-wheel, controlled by a dedicated *in-house built electronic module* in the NIM standard. The controller allows adjustments of the time interval in powers of 2, up to 4096 seconds, and provides several output signals which can be used in the data acquisition system: logic TTL signals for tape start (to tag the moment a new implantation point moves towards measurement) and logic gate signals for tape movement (which can be used to inhibit the acquisition during the transportation phase). An interface with the pulsing system of the 9-MV Tandem [7] is also present, however it was not used during the course of this work. Current configuration has a transit time of  $\sim 1.5$  seconds. Both measurement and implantation intervals have the same duration, i.e. while a radioactivity spot is in the detection area, another spot is subject to implantation. Interval optimization is extensively discussed in [12] and will not be addressed in this work. After a measurement interval, the activity spot continues on to a recirculation box (or delay box) where it loops back and forth on a series of roller pulleys. This ensures that other possible longer-lived nuclei will not decay in the measurement area, which would result in spectra contamination.

The recirculation box also houses a platform with two spring-loaded arms that keep the tape under tension, as well as an off-switch which acts as a fail-safe (i.e. shuts down the stepper motor). The entire system is a closed-loop, with the tape amounting a length of  $\sim 35$  m. Reduced-background conditions are ensured by placing the setup near the wall separating Target Halls 1 and 2 of the Tandem building. The wall acts as an optimum shield between the measurement point and the production and recirculation points, as the latter two behaving as continuous sources of  $\gamma$ -rays over the course of an experiment.

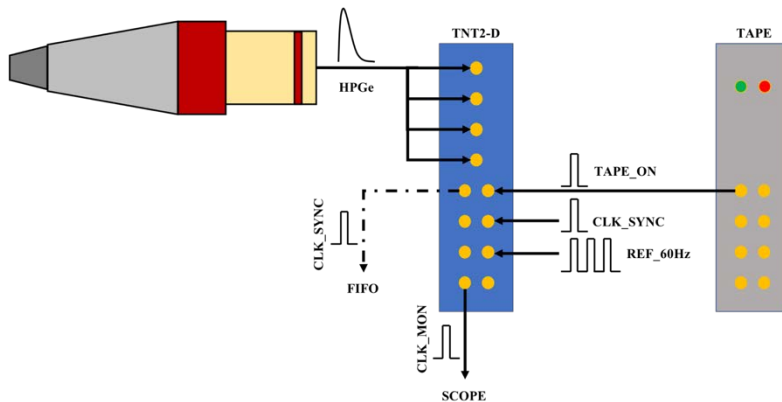


Fig. 2 – Block-scheme of the typical acquisition system for one BGO-suppressed Clover detector. Detector signals are fed directly to the inputs of the digitizer cards. The tape controller provides reference signals. See text for details.

The associated measurement station from Target Hall 2 is comprised of a goniometric table with three Compton-suppressed clover detectors and a digital data acquisition system based on XIA DGF-4C rev.F digitizers [10] and TNT2-D digitizers [11]. Data is acquired trigger less and is sorted using an in-house developed event builder.

The acquisition system, represented in Fig. 2, uses a minimum number of modules, as follows: The tape controller which provides two independent outputs for TAPE\_ON (i.e. start of tape movement for each cycle, taken as a time reference), several digitizer cards in master-slave configuration (where the preamplifier signals are fed directly to the digitizer input and a CLK\_SYNC -clock synchronization signal- output only from the master card is fed to a CAEN N454 4-8 Logic FIFO, multiplied, then re-injected in both master and slave cards, in order to synchronize data offline) and one CAEN NDT6800 digital signal emulator, which provides two outputs configured to feed 60 Hz TTL signals (REF\_60Hz) to each card, as a reference for deadtime correction.

### 3. Test Experiments and Commissioning

Two experiments have been performed to assess the performance of the new decay setup. The first experiment involves a heavy-ion induced fusion-evaporation reaction aimed at strictly testing the transportation capability of the setup. The second one investigated the feasibility of the setup for measuring half-lives of  $\beta$ -decaying nuclei as alternate tests of the Standard Model [18]. Both experiments employed the TNT2-D digitizers.

#### 3.1. Assessing the transportation capability of the decay station

A short proof-of-concept experiment was conducted using the first iteration of the setup in order to test its' functionality. A  $\approx 0.67 \text{ mg/cm}^2$  thick self-supported  $^{58}\text{Ni}$  target and a  $^7\text{Li}$  particle beam at an energy of 22 MeV were used for the reaction. While PACE4 [13][14] and NRV [17] calculations revealed a broad range of residual nuclei (Figure 3), with half-lives spanning several orders of magnitude,

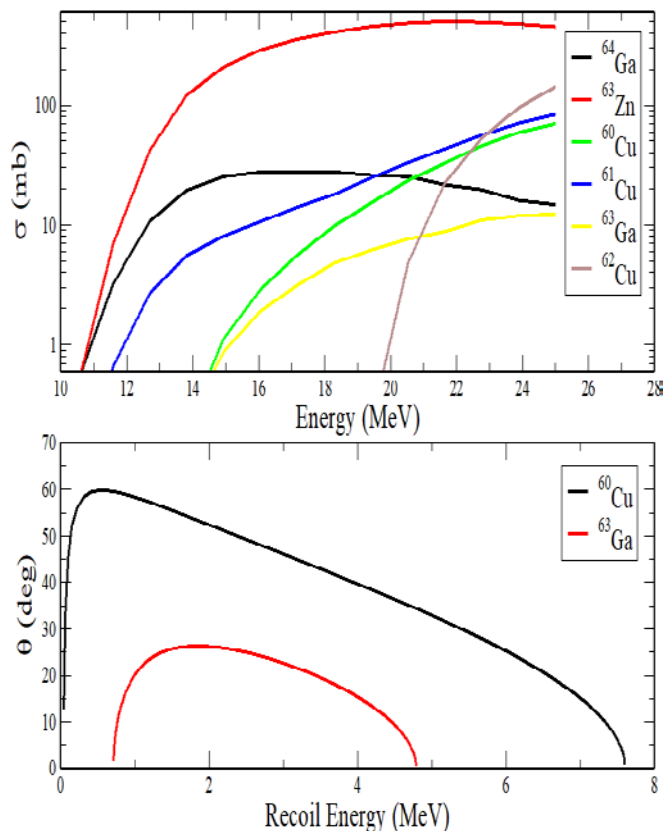


Fig. 3 – Calculated angular distributions for nuclei of interest, at an optimum beam energy of 22 MeV (lower panel), derived from calculated cross-sections (upper panel) using PACE and NRV

only two were selected to verify the transportation and separation capacity:  $^{63}\text{Ga}$  ( $T_{1/2}=32.4$  s)  $\rightarrow$   $^{63}\text{Zn}$  and  $^{60}\text{Cu}$  ( $T_{1/2}=23.7$  m)  $\rightarrow$   $^{60}\text{Ni}$ .

Associated kinematics calculations were performed for all exiting channels and the broadest calculated angular distribution was used to capture all possible nuclei; therefore no geometrical optimization was undertaken in this case. Separation between nuclides was performed only by sequencing tape movements, at intervals according to [12]. By using the tape-start signal as a timing reference, the decay curves for each individual cycle can be obtained, resulting in a sawtooth-shaped time spectrum. Data was recorded in singles mode, to identify all possible  $\gamma$ -ray transitions during the experiment, including a background estimate. As a consequence, all possible  $\gamma$ -rays from the natural background will be recorded alongside the  $\gamma$ -rays from the decays, as can be seen in the middle and lower panel of Figure 4.

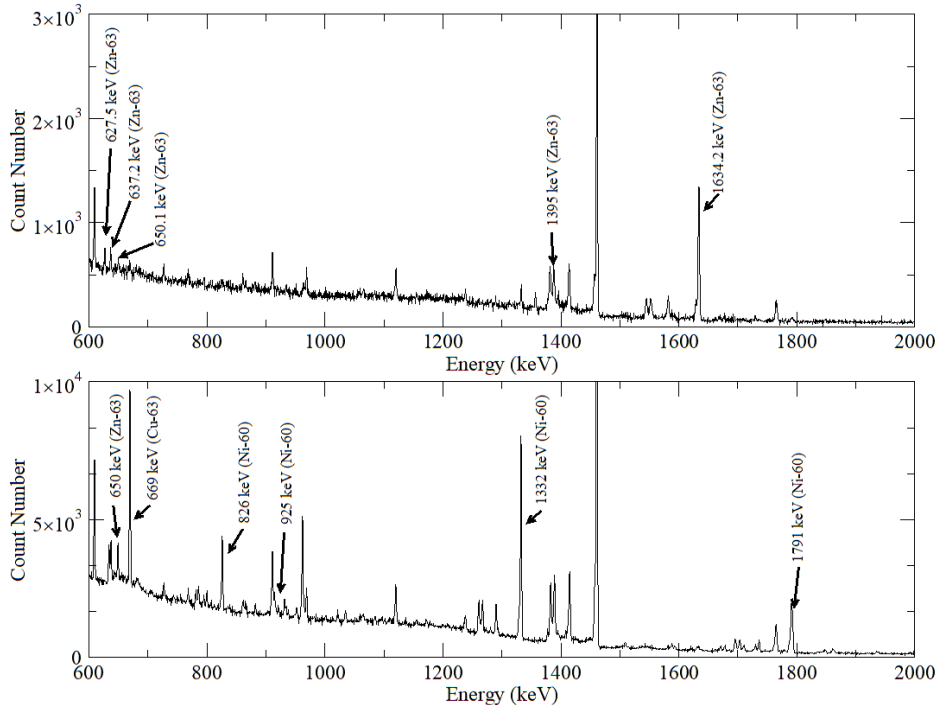


Fig. 4 –  $\gamma$ -ray spectrum for  $^{63}\text{Zn}$  in a 58 sec tape cycle (upper panel), and the  $\gamma$  spectrum for  $^{60}\text{Ni}$  in a 43 min cycle (lower panel)

### 3.2 Assessing the tape station for half-life measurements

The second experiment was aimed at testing the possibility of measuring half-lives of  $\beta$ -decaying nuclei. Precise values for  $T_{1/2}$  of super allowed and  $\beta$  decays prove to be alternate tests of the unitarity of the CKM matrix of the Standard

Model [18][19], as they reveal key information regarding the up-down quark-mixing element,  $V_{ud}$ , in the Conserved Vector Current (CVC) hypothesis [18][19]. It implies that a corrected  $F_t$  value as [19] must be determined, achievable through mass, branching ratio and half-life measurements. The focus of the present work is on the former. Systematic surveys [18][20] of  $\beta$  decay data related to mirror isospin doublets reveal  $^{27}\text{Si}$  as having the largest discrepancies and uncertainties in terms of measured half-life values, with an  $T_{1/2}$  of 4.135(15) seconds averaged over a large number of reported experiments.

The half-life of  $^{27}\text{Si}$  was measured using the newly-commissioned tape station via  $^{24}\text{Mg}(^{4}\text{He}, n)^{27}\text{Si}$  reaction, with two clover detectors in coincidence, placed at  $180^\circ$  between each other, in order to detect the 511 keV  $\gamma$ -rays following  $\beta^+$ -driven pair-annihilation. An isotopically-enriched self-supported  $^{24}\text{Mg}$  target of  $\sim 350 \mu\text{g/cm}^2$  thickness was used. NRV [17] and TALYS [23] calculations indicate an optimum beam energy of 17.5 MeV for maximizing the  $^{27}\text{Si}$  cross-section, as shown in Fig. 5. Prior to  $^{27}\text{Si}$ , a test experiment was performed, using the reaction  $^{27}\text{Al}(^{4}\text{He}, p)^{30}\text{P}$ , with a  $\approx 0.5 \text{ mg/cm}^2$  thick target at a beam energy of 17.5 MeV, with a target-to-tape distance of  $\approx 3 \text{ cm}$ , with one collimator upstream of the target, and an aperture of  $\phi = 2.5 \text{ mm}$ .

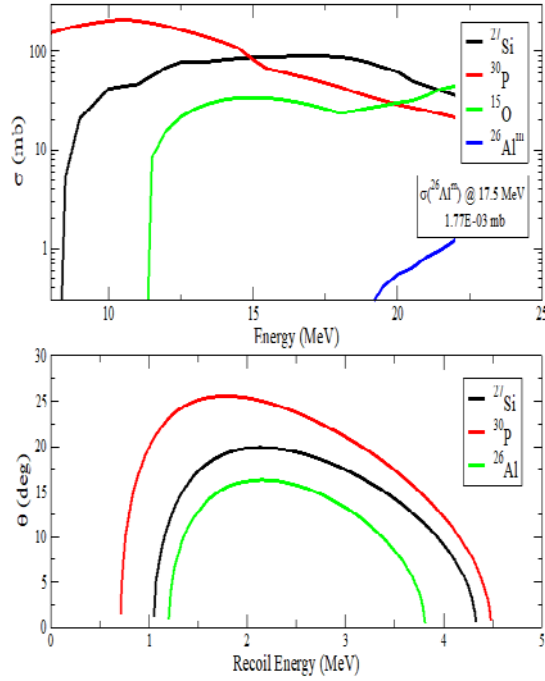


Fig. 5 – Calculated angular distributions at a beam energy of 17.5 MeV (lower panel) derived from the cross-sections (upper panel) for half-life measurement experiments. The angular distribution is calculated for  $^{26}\text{Al}$  as total, whereas the cross-section is only of the isomer. Only  $\beta$ -unstable species are shown.

The known half-life of  $^{30}\text{P}$  is 2.498(4) minutes (149.88 seconds), according to [28], and as a consequence the total tape cycle was set to 304 seconds. Data was recorded trigger less using the acquisition system presented in Fig. 2 and was sorted in both singles and coincidence mode. The corresponding singles spectrum for the  $^{30}\text{P}$  experiment is shown in Figure 6, along with the time spectrum.

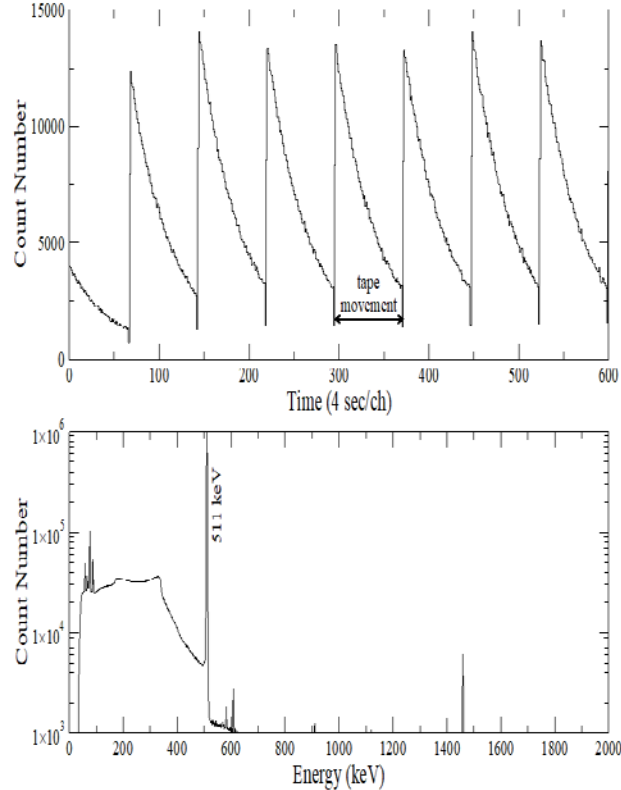


Fig. 6 – Sawtooth-shaped time spectrum with associated singles spectrum recorded for  $^{30}\text{P}$ . A dominating 511 keV transition corresponding to pair-annihilation can be seen, as expected

After resorting data in coincidence mode, and gating on the 511-keV transition, the resulting saw-teeth time spectra were algebraically summed on an interval basis, leading to a total decay curve for the entire experiment. Initial one-component half-life analysis of  $^{30}\text{P}$  reveals (Fig. 7) a half-life of 127.33 seconds, well below the expected 149.88 seconds, with no known corresponding nuclide. Beam-tape interaction was taken into account, and data was treated as a two-component decay. Given the chemical composition of the tape [24] and the beam energy, and considering isotope ratios, PACE and NRV calculations pinpoint  $^{12}\text{C}(^{4}\text{He}, \text{n})^{15}\text{O}$ , which further decays to  $^{15}\text{N}$  through  $\beta^{+}$  as a contaminant, its half-life being 122.24 seconds [26].

Two-component decays given by individual contributions, as time-dependent functions

$$f(t) = N_1 \exp(-\lambda_1 t) + N_2 \exp(-\lambda_2 t) \quad (1)$$

can be rewritten in terms of effective activity and effective decay rates (effective half-lives)

$$f(t) = N_{eff} \exp(-\lambda_{eff} t) \left[ \frac{N_1}{N_{eff}} \exp(\lambda_{eff} - \lambda_1) t + \frac{N_2}{N_{eff}} \exp(\lambda_{eff} - \lambda_2) t \right] \quad (2)$$

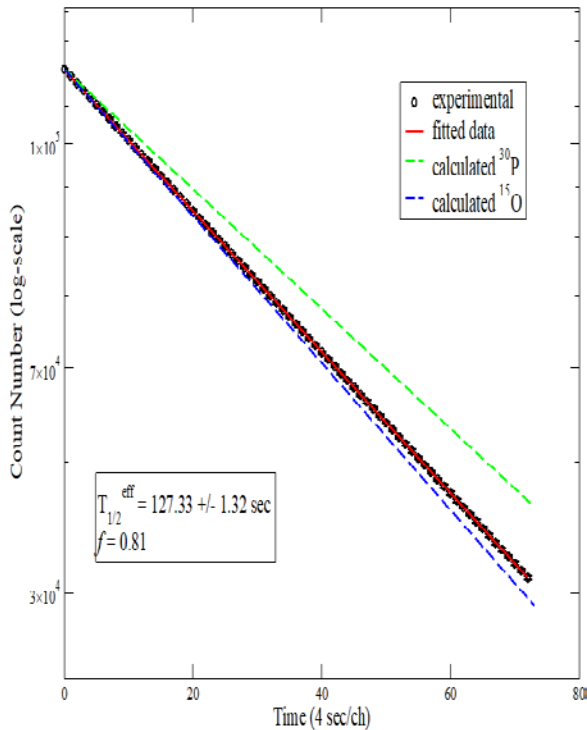


Fig. 7 – Measured time-decay spectrum for the total data obtained in the  $^{30}\text{P}$  beam test, on a semilog scale, spanning an interval of 304 seconds. The dashed lines show the calculated contaminants as opposed to the decay of interest. Note that the points were shifted to  $t=0$ , with the tape movement being removed.

Using a series expansion of the exponential functions, neglecting terms from the second order up, and considering the effective activity as a sum of its' components, with known decay rates (or half-lives)  $\lambda_{1,2}$ , data can be analyzed using the total count number recorded in a specific time interval, and can further estimate the amount of one component relative to another, by using a nonlinear least-squares fit to the function

$$\lambda_{eff} = f\lambda_1 + (1 - f)\lambda_2 \quad (3)$$

in which  $f$  is the ratio between two decay rates, and can be used to obtain the fraction of one contaminant (i.e.  $\lambda_1$ ) from a measurement on  $\lambda_2$ . The results of this analysis are shown in the lower-left corner of Fig. 7, indicating a ratio of 0.81 of contamination. Consequently, modifications of the collimators and the beam plug were performed to reduce possible contamination during the  $^{27}\text{Si}$  measurement.

Data for the latter was analyzed in a similar manner, however, the final decay curve reveals several components:

$$f(t) = [N_{27\text{Si}} \exp(-\lambda_{Si}t) + N_{26\text{Al}} \exp(-\lambda_{Al}t)]_{fast} + N_{slow} \exp(-\lambda_{slow}t) \quad (4)$$

in which the first term corresponds to the expected  $^{27}\text{Si}$  [27] and  $^{26}\text{Al}^m$  [25] contributions (short), followed by a long-lived component. In order to isolate the long contribution, numerical differentiation was used, as shown in Figure 8,

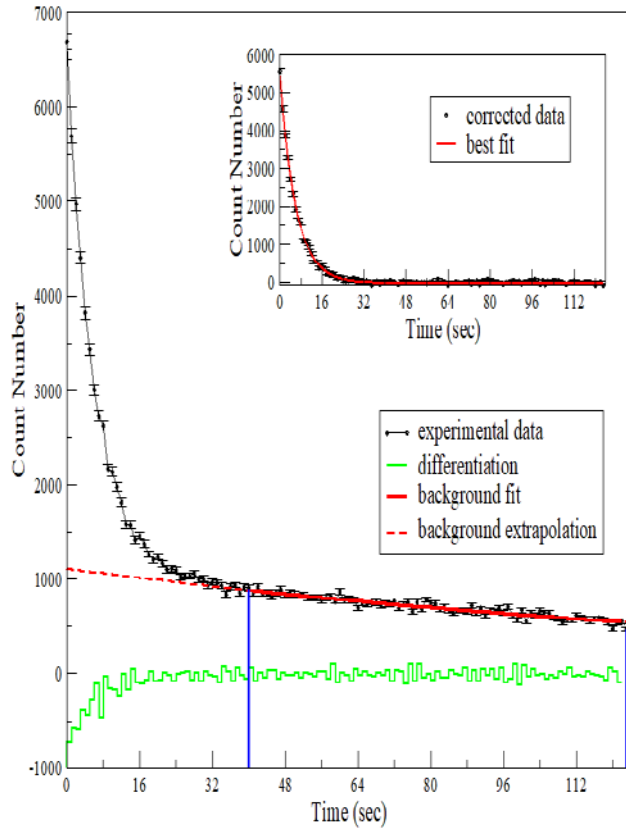


Fig. 8 – Analysis procedure for one time-aligned run containing the total decay data.

until reaching a plateau. The lower and upper limits of the plateau (marked with blue) were used as constraints for an exponential fit to extract the half-life of the

contaminant. This was further extrapolated then subtracted from the total decay curve, resulting in a corrected curve (upper-right inset). From this point, the same method was applied as for  $^{30}\text{P}$ . Data was analyzed on a run-by-run basis, with the results shown in Fig. 9.

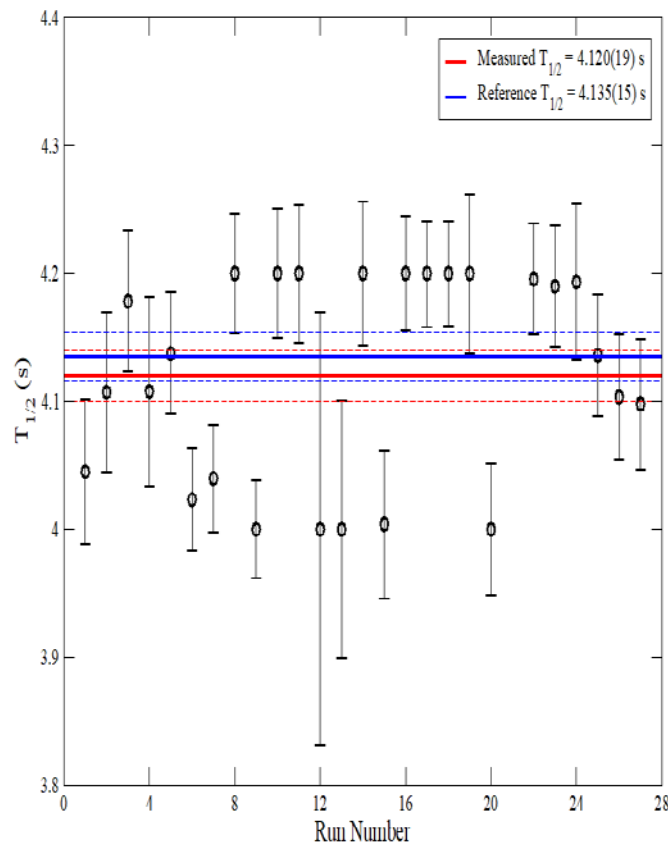


Fig. 9 – Half-life of  $^{27}\text{Si}$  determined from the run-by-run analysis. Reference data is indicated with dark blue, while the final measured value is marked with red. The solid lines indicate the average value, with  $1\sigma$  uncertainty (dashed lines).

The final value for the half-life of  $^{27}\text{Si}$  was obtained by averaging the results of each run, leading to a value of 4.120(19) seconds, in agreement with the most recent and most precise value reported by Magron *et al.* [29].

## 6. Conclusions and outlook

A new experimental setup has been commissioned at the 9-MV Tandem accelerator at IFIN-HH, consisting of a radioactivity transport station and a high-

efficiency detection array equipped with digital electronics. The setup has been tested by measuring the  $\beta$  decay of several isotopes, aiming at spectroscopic and half-life measurements.

The goniometric platform makes it ready to study various aspects of nuclear structure by means of linear  $\gamma$ -ray polarization and angular correlation experiments in the rare-earth region.

The future addition of a quadrupole lens along the beamline will improve the beam optics, minimize the beam scattering on the stopper, thus reducing possible contamination.

## R E F E R E N C E S

- [1] *W. D. Hamilton* (ed.), The Electromagnetic Interaction In Nuclear Spectroscopy, North-Holland, 1975
- [2] *D. Bucurescu, Gh. Căta-Danil, N. V. Zamfir*, Nucl. Phys. News **17** (2007), 1
- [3] *N. V. Zamfir*, AIP Conf. Proc. **899**, 23 (2007)
- [4] *R. Bass*, Nuclear Reactions with Heavy Ions, Springer-Verlag, 1980
- [5] *N. Mărginean* et al., Eur. Phys. J. A (2010) **46**, 329-336
- [6] *D. Bucurescu* et al., Nucl. Instr. Meth. Phys. Res. A **837** (2016), 1-10
- [7] *S. Dobrescu* et al., AIP Conf. Proc. **1099** (2009), 51
- [8] *N. V. Zamfir, R. F. Casten*, J. Res. Natl. Inst. Stand. Technol. **105** (2000), 147
- [9] *G. Duchene* et al., Nucl. Instr. Meth. Phys. Res. A **432** (1999), 90-110
- [10] *W. D. Warburton* et al., Appl. Rad. Iso. **53**, Issue 4-5 (2000), 913-920
- [11] *L. Arnold* et al., IEEE. Trans. Nucl. Sci. **53** (2006), 3
- [12] *M. A. Caprio*, Structure of collective modes in transitional and deformed nuclei, PhD Thesis, Yale University, 2003
- [13] *O. B. Tarasov, D. Bazin*, Nucl. Instr. And Meth. B **204** (2003), 174-178
- [14] *O. B. Tarasov, D. Bazin*, Nucl. Instr. And Meth. B **266** (2008), 4657-4664
- [15] *J. Mierzejewski* et al., The COMPA Manual, <http://www.old.slcj.uw.edu.pl/~jmierz/compa.pdf>
- [16] *J. F. Ziegler* et al., Nucl. Instr. And Meth. B **268** (2010), 1818-1823
- [17] *A. V. Karpov* et al., Yadernaya Fizika, 2016, Vol. **79**, No. 5, pp. 520–532
- [18] *J. C. Hardy, S. Towner*, Ann. Phys. **525**, 443 (2013)
- [19] *J. C. Hardy, S. Towner*, Phys. Rev. C. **91**, 022501 (2015)
- [20] *N. Severijns, O. Naviliat-Cuncic*, Ann. Rev. Nucl. Part. Sci. **61**, 23 (2011)
- [21] *N. Severijns, M. Beck*, Rev. Mod. Phys. **78** July-Sept 2006
- [22] *N. Severijns, M. Tandecki, T. Phalet, and I. Towner*, Phys. Rev. C **78**, 055501 (2008)
- [23] *A. J. Koning* et al., AIP Conf. Proc. **769**, 1154 (2005)
- [24] *M. J. Berger* et al., NIST Standard Reference Database 124 (July 2017)
- [25] *M. S. Basunia, A. M. Horst*, Nuclear Data Sheets for A = 26, Vol. **134**, 1-148 (2016)
- [26] *F. Ajzenberg-Selove*, Nucl. Phys. A, Vol. **523**, Issue 1, 1-196 (1991)
- [27] *M. Basunia*, Nuclear Data Sheets for A = 27, Vol. **112**, Issue 8, 1875-1948 (2011)
- [28] *M. Basunia*, Nuclear Data Sheets for A = 30, Vol. **111**, Issue 9, 2331-2424 (2010)
- [29] *C. Magron* et al., Eur. Phys. J. A (2017) **53**: 77